Hindawi
Journal of Nanomaterials
Volume 2020, Article ID 5045637, 12 pages
https://doi.org/10.1155/2020/5045637

Research Article

Electrospun Polystyrene/LDH Fibrous Membranes for the Removal of Cd^{2+} Ions

Mohamed A. Alnaqbi, Joel A. Samson, and Yaser E. Greish

Department of Chemistry, College of Science, United Arab Emirates University, Al Ain, UAE

Correspondence should be addressed to Mohamed A. Alnaqbi; m.alazab@uaeu.ac.ae and Yaser E. Greish; y.afifi@uaeu.ac.ae

Received 16 September 2019; Revised 23 November 2019; Accepted 5 December 2019; Published 5 March 2020

Academic Editor: Leander Tapfer

Layered double hydroxides (LDHs) have been extensively studied for a broad range of applications because of their ease of synthesis and chemical modifications. The chemical and crystal structure of LDH provides opportunities of combination with polymers forming nanocomposites. In the current study, MgAl-LDH particulates have been incorporated into micro- and nanofibers of polystyrene (PS) using an electrospinning processing technique of their respective homogeneous solutions. The effect of the varying proportions of LDH and PS on the structure, morphology, and thermal properties of the fabricated LDH-PS fibrous membranes has been investigated. The potential application of the optimally fabricated LDH-PS fibrous membranes in the removal of Cd^{2+} ions from aqueous media has been evaluated as well. Results showed the possibility of loading the PS fibrous membranes with up to 60 wt% of LDH particulates, which in turn modified the thermal stability and integrity of the produced fibrous membranes. Due to the high hydrophobicity of the PS fibrous matrix, no changes in the crystal structure of the LDH inclusions were observed. Both as-prepared LDH particulates and optimally prepared LDH-PS fibrous membranes showed a high potential for the removal of Cd^{2+} ions from aqueous media. This is attributed to a cation-exchange mechanism involving the adsorption of Cd^{2+} ions from a solution with the preferential leakage of Al^{3+} ions from the crystal structure of LDH.

1. Introduction

The concept of improving the distinctive features of conventional polymers, such as mechanical strength, biodegradability, thermal stability, and hydrophobic nature, fuels the research interest in developing polymer-based composites using particulate additives of various sizes (macroscale to nanoscale) [1–3]. One of the approaches that has been extensively studied lately is to design nanofibrous composites that will have the advantage of a high surface area of its fibers as well as close proximity between the polymer matrix and the fillers at the nanoscale. The structure of the polymeric matrix and the filler dictates the properties and applications of the fabricated composites. Among the known inorganic fillers, the addition of layered double hydroxide (LDH) to a polymer widens the scope of the applications of the produced composites. LDHs have found a wide range of applications, such as adsorption [4], separation [5], energy storage [6], corrosion protection [7], drug delivery [8], catalysis [9], and flame retardation [10].

Understanding the functional properties of LDH within various polymer matrices will contribute to improving the biodegradability, thermal resistance, and functionality of the resulting LDH-polymer composites [11, 12]. First discovered in 1842 [13], LDH is an intercalation anionic clay-like solid that is also known as hydrotalcite [14] and is represented by a general chemical formula $[M^{II}_{(1-x)}M^{III}_{x}\ (OH)_2]^{x+}\ (A^{n-})_{x/n}\ mH_2O$, where "$M^{II}$" denotes divalent metal ions (Mg^{2+}, Cu^{2+}, Ni^{2+}, etc.), "M^{III}" denotes trivalent metal ions (Al^{3+}, Cr^{3+}, etc.), and "A" denotes anionic species with valency n (Cl^-, SO_2^-, and CO_3^-). A schematic diagram showing the detailed structure of a typical LDH [15] is shown in Figure 1.

A typical LDH structure consists of closely grouped hydroxyl anions surrounding the central metal ion in an octahedral and hexahedral lattice arrangement. Their layered sheets are constructed by hydrogen bond interaction which can interconnect the anionic species and water molecules within the interlayer space lattice [16]. LDH has the capacity to incorporate ionic species within the interlamellar spacing. Well-crystallized LDH materials are often synthesized by

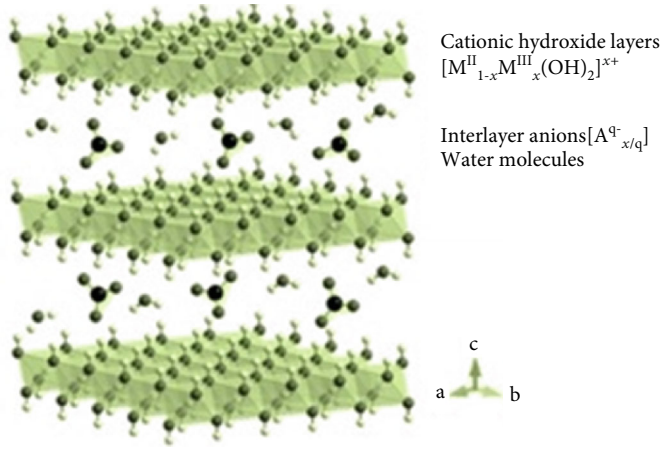

Figure 1: A schematic representation of a typical LDH structure [15].

coprecipitation [17], hydrothermal synthesis [18], or a combination of both methods [19], with a high degree of reproducibility in all methods. Moreover, a scalable continuous process was developed to prepare ultrafine LDH nanoparticles using continuous-flow hydrothermal reactors [20]. Other methods were also explored to prepare LDH, where a LDH-like reactant is used as a template. These methods include anion exchange, dissolution crystallization, and dissociation deposition diffusion [21].

A combination of LDH and polymer in a nanocomposite has been found to produce superior properties where the physical, thermal, electrical, magnetic, optical, and mechanical properties of the polymer are enhanced [22–28]. LDH-polymer nanocomposites are fabricated by blending or intercalation in solution [29] or in a molten state [30] of the polymer, through in situ polymerization, through in situ formation of LDH [31], or through double in situ polymerization [32] and LDH formation methods [33]. Apart from the molten blending, homogeneous nanocomposites can be prepared. In a homogeneously formed nanocomposite, exfoliation of the LDH layers may take place, where polymeric chains can be arranged between the layered structures [34]. Exfoliation mostly occurs if the polymeric chains are hydrophilic in nature that will interact with the ionic species within the interlamellar spacing. This process takes place during solution blending due to the lower viscosity of the solution than the melt which allows the LDH layers to be exfoliated by the polymer chains that are dispersed in solution. Hydrophobic polymers, on the other hand, do not exfoliate the LDH structure unless an organic linker, such as a surfactant, is used [35].

In the current study, a MgAl-LDH and polystyrene will be homogeneously blended in a solution and will be further processed into a fibrous composite membrane using an electrospinning technique. A number of fiber-making processing methods are known [36–39], but electrospinning is characterized by its robustness. Fibrous membranes made by electrospinning feature the flexibility of design and the interconnectivity of its porosity as well as the high surface area of the fibers by virtue of the small size (nm-μm) of the fibers. Unlike functionalized nonfibrous polymer membranes [40], the characteristics of fibrous membranes make them feasible to be used for water treatment [41]. In an LDH-polystyrene fibrous composite membrane, a polystyrene fibrous structure will provide the skeleton of the membrane and will help in the removal of sub-μm solid particulates from water [42], while the LDH solid particles will act on the removal of soluble pollutants from water.

LDH-based materials have been widely used in the cleanup of soluble anionic pollutants in water, such as nitrates [43] and phosphates [44]. This application has been attributed to the diversity and functionality of the interlayer region, in the LDH structure, that contains easily exchangeable intercalated anions and solvation molecules with hydrogen bonds. Moreover, the ability of LDH to remove soluble heavy metal ions was also explored [45]. However, regeneration of LDH and their agglomeration in solution restrict their application in water treatment [46], unless compounded with other materials in the form of functional composites that will minimize these shortcomings [47].

The removal of soluble heavy metal contaminants from water takes place through ion exchange or precipitation [48]. Ion exchange takes place through the replacement of one of the metal ions of the LDH by the metal ion pollutant. Examples include the replacement of Mg^{2+} ions in a MgAl-LDH [49] or Ca^{2+} ions in a CaAl-LDH [50] by Zn^{2+} ion pollutants. Lead (Pb^{2+}) ions, on the other hand, were removed from water by precipitation due to the increase in the pH of the aqueous medium as a result of LDH partial dissolution [51]. In general, there are still a limited number of publications reporting the cationic exchange capabilities of LDH.

In this current study, the formation and characterization of fibrous membranes of a polystyrene (PS) polymer matrix and the inclusion of MgAl-LDH particulates in the matrix, as a function of the relative proportions of the PS and LDH components of the membranes, are presented. Optimally prepared fibrous membranes have been also preliminarily evaluated for their potential as sorbents of Cd^{2+} ions from aqueous media.

2. Methods and Materials

2.1. Materials. Polystyrene (Aldrich) and N,N-dimethylformamide (DMF, Sigma-Aldrich) were used to prepare the

initial polystyrene solution for electrospinning. The hydrate forms of magnesium nitrate ($Mg(NO_2)_2{\cdot}6H_2O$, Panreac) and aluminum nitrate ($Al(NO_2)_3{\cdot}9H_2O$, Riedel-de Haen) were used as precursors for the LDH synthesis. An aqueous solution of sodium hydroxide (NaOH, Aldrich) was prepared to maintain a high basic pH for LDH preparation. $Cd(NO_3)_2{\cdot}4H_2O$ (Sigma-Aldrich) was used for the initial evaluation of LDH and its composites for the removal of Cd^{2+} ions.

2.2. Synthesis of MgAl-Layered Double Hydroxide. By a co-precipitation method, $Mg(NO_2)_2.6H_2O$ and $Al(NO_2)_3.9H_2O$ were used as precursors in the synthesis of MgAl-layered double hydroxides (MgAl-LDHs) at the ratio of 3 : 1 (Mg : Al). In a typical experiment, the powder precursors were dissolved in 100 ml of distilled water, in a 250 ml flask, then purged in the N_2 atmosphere and refluxed at 80°C while maintaining the pH of the solution at (pH ~10) by a dropwise addition of NaOH (2.5 M) solution. This reaction was carried out for 24 hrs. The resultant slurry was washed thoroughly with distilled water to remove the excess NaOH and dried at 60°C for 24 hrs in a vacuum oven. The MgAl-LDH (white) powder was ground to obtain a fine homogeneous powder.

2.3. Fabrication of Polystyrene LDH Fiber Composites. LDH-containing PS solutions were prepared by suspending LDH powders in a 5, 10, and 20 wt% PS in DMF. In order to obtain a homogeneous suspension of each of the LDH-PS formulations, a predetermined weight of LDH fine powder was first suspended in DMF followed by dissolving the PS granules at room temperature until a homogeneous suspension was obtained. Based on our preliminary studies, the following LDH-PS formulations were prepared to be electrospun to nonbeaded fibrous morphology:

5% PS: 30, 40, 50, and 60 wt% LDH
10% PS: 5, 10, 20, 30, and 40 wt% LDH
20% PS: 5 and 10 wt% LDH

An electrospinning technique was used for making LDH-PS composite fibrous membranes. In a typical experiment, a volume of 10 ml of each of the abovementioned formulations was electrospun at ambient conditions, an operating voltage of 20-25 kV, a feeding rate of 1 ml/hr, and a spinning distance of 15 cm. Collected LDH-PS composite membranes were dried in air to be characterized and evaluated.

2.4. Characterization and Evaluation. The effect of the addition of LDH on the viscosity of the LDH-PS homogeneous suspensions was studied as a function of the concentration of LDH using a Brookfield viscometer (LV DV-II+Pro EXTRA) by Spindle-S34 at 50 rpm. A powder X-ray diffraction technique (Shimadzu XRD-6100, Japan) was applied to confirm the structure and crystallinity of the prepared, pristine LDH and the LDH-PS composite membranes. An IR spectroscopy technique (Thermo-Nicolet (NEXUS-470), USA) was used to further evaluate the structure of the prepared LDH powder as well as the electrospun PS fibers and their composite membranes. IR spectra were collected using an attenuated total reflectance (ATR) mode. The thermal analysis of the pure LDH, PS, and their electrospun composite membranes was further carried out using a Shimadzu thermogravimetric analysis (TGA-50) and differential scanning calorimeter (DSC-60) with the heating range set between 30 and 600°C, with the gradual heating rate of 20°C/min. The morphological characteristics of the gold-coated pure LDH powder, PS fibers, and their composite fibrous membranes were studied using a scanning electron microscope (SEM, Oxford Instruments, UK) at an operating voltage of 15 kV (Beam Voltage). The effect of the addition of LDH on the hydrophobic nature of the LDH-containing PS fibers was investigated by the measurement of their water contact angle (DM-301, Kyowa Interface Science Co.) at 25°C.

To preliminarily evaluate the potential of the prepared LDH-PS fibrous membranes for the removal of heavy metal ions from waste water, a simulated aqueous medium was used containing 60 ppm aqueous solution of $Cd(NO_3)_2$. This concentration presumes a highly contaminated waste compared with the WHO-permitted concentration of Cd^{2+} ions in drinking water of 0.003 ppm. LDH-PS fibrous membranes containing the highest [LDH] were utilized for this experiment. A 0.1 g of each of the fibrous membranes was soaked in 10 ml of the Cd^{2+} ion solution and kept at 25°C with continuous stirring for up to 12 hours. Aliquots were collected after predetermined time periods, filtered using a 0.22 μm cellulose acetate microfilter, and then analyzed for the concentration of Cd^{2+} ions remaining after each time point. A control experiment was also conducted where 0.1 g of pristine finely ground LDH powder was used. Analysis of $[Cd^{2+}]$ was carried out using an inductively coupled plasma-atomic emission spectroscopy (ICP-AES) after calibration, using a Cd^{2+} standard solution.

3. Results and Discussion

3.1. Characterization of LDH-PS Fibrous Sorbents. Figure 2(a) shows the XRD pattern of the MgAl-LDH that was synthesized in the current study. All peaks were correlated with standard known crystallinity of LDH [11]. Diffraction peaks of MgAl-LDH were confirmed by the lamellar indices (003), (006), (009), and (110), whereas peaks observed at 2θ values of 11.3°, 22.8°, 34.5°, and 55.5° determine the molecular arrangements of the metallic centers of the layered structure, Mg/Al (3 : 1). The standard basal reflections (003) and (006) determine the octahedron- and hexahedron-layered arrangement of metal hydroxides (M-OH), similar to the structure of hydrotalcite and brucite clay minerals. The calculated interlayer distance of $d_{(003)}$ was 7.7 Å (approx. 0.7 nm). The interlayer distance was determined by the presence of the competing carbonate and nitrate anions, as shown in the IR spectrum of the prepared LDH (Figure 2(b)). The variation in ionic radii and electron affinity towards the hydroxyl layers alters the interlamellar distance. The high intensity of the diffraction peak determines the crystalline nature of the di-metal-structured layers. The IR spectrum of the as-prepared LDH powder in Figure 2(b) shows a typical spectrum of a pure LDH phase. A broad absorption band observed at 3492.3 cm^{-1} is attributed to the presence of -OH (stretch) vibration, while the presence of interlayer water molecules (H-OH) was confirmed at 1648.9 cm^{-1}. The sharp peak at 1345.5 cm^{-1} denotes

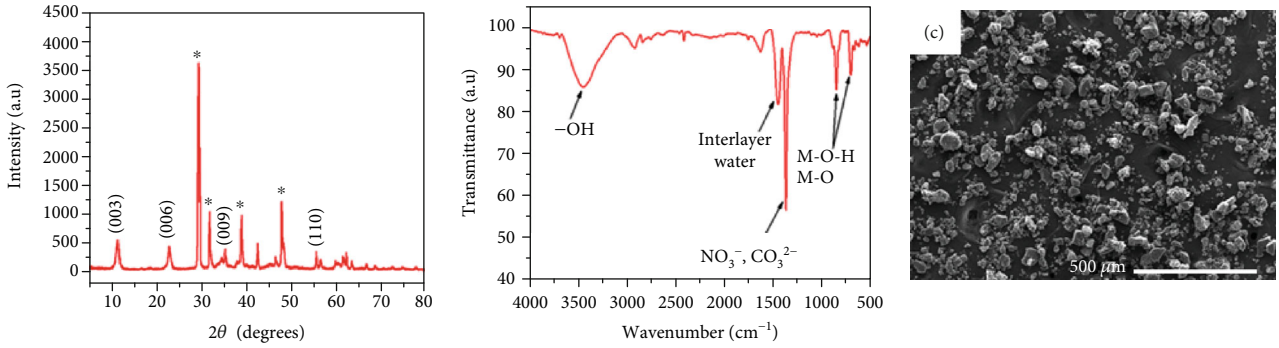

FIGURE 2: X-ray diffraction pattern (a), infrared spectrum (b), and scanning electron micrograph (c) of the as-prepared MgAl-LDH particulates.

the availability of oxide anions (NO_3^- and CO_3^{2-}) within the interlamellar space of LDH. The metal hydroxide vibrations (M-O-H and M-O) appear at 836.3 cm^{-1} and 658.8 cm^{-1}, respectively [52]. Both XRD and IR results hence confirm the structural purity and crystallinity of the synthesized LDH. Figure 2(c) demonstrates the morphology of the as-prepared LDH powder. Porous agglomerates of the irregular-shaped LDH particulates, with an average size of 1.5 μm, were observed. These are formed as a result of the removal of the volatile ingredients, used during the precipitation of LDH, under vacuum.

In comparison, Figure 3(a) shows the IR spectrum of the as-prepared electrospun PS fibers, where bands characteristic to PS were observed at 3024.4 cm^{-1} and 2922.2 cm^{-1}, confirming the C-H (aromatic) tension and -CH_2 (asym./sym.) tension of the polymeric chain extension. The C=C (aromatic) stretch was indicated at 1642.2 cm^{-1}, while the -CH (bending) vibration of the methylene group was indicated at 1490.9 cm^{-1} and 1450.5 cm^{-1}. The C-H (bending) of the monosubstituted benzene derivative, at 754.2 cm^{-1} and 698.2 cm^{-1}. The presence of these bands confirms all functional vibration modes of a standard PS composition and indicates its phase purity and stability after electrospinning. Figure 3(b) shows an SEM image of the as-electrospun PS microfibers, where fibers averaging at 5 μm, with a homogeneous fiber size distribution and interconnected porosity were observed. The insert in Figure 3(b) indicates the smooth surface of the as-electrospun PS fibers.

The fiber-making ability of the LDH-PS composite suspensions was investigated by SEM analysis, where nonbeaded fibers were considered while composite mixtures that resulted in other morphologies were excluded. These preliminary observations limited the proportions of LDH in each of the PS solutions prepared for electrospinning. LDH-containing PS homogeneous suspensions showed a variable degree of viscosity unlike that of their respective LDH-free PS solutions, as shown in Figure 4. A significant difference in the viscosities of the pure PS solutions was found. A solution containing 20 wt% PS exhibited a viscosity of 177 cP. Decreasing the proportion of PS in the solution to 5 and 10 wt% showed a dramatic decrease in the viscosity reaching 5.7 and 21.4 cP, respectively. Increasing the LDH loading resulted in a slow increase in the viscosities of the resultant suspensions, which is attributed to the disturbance of the homogeneous flow of the PS solutions with the addition of the DMF-insoluble LDH particulates.

The structural morphology and the elemental analysis of the electrospun LDH-PS fibers were recorded, as shown in Figures 5–8, for LDH-PS fibrous membranes made of solutions containing 5, 10, and 20 wt% PS in DMF, respectively. Compared with a homogeneous fiber size distribution of pure PS solutions as shown in Figure 3(b), all LDH-PS composite fibers showed a heterogeneous fiber size distribution. Moreover, a pronounced increase in the surface roughness of the composite fibers was also observed. This was also accompanied by an increase in the contact angle of the composite fiber surfaces, as shown in the inserts of all micrographs. This is attributed to the presence of the LDH particulates with their hydrophobic surfaces onto and into the PS fibers, while the hydrophilic layer that is made of the hydroxyl carbonate or nitrate groups is entrapped within the LDH crystalline sheets. Due to the significantly lower viscosity of the LDH-PS fibers electrospun from solutions containing 5 wt% PS, LDH particulates were found onto the surfaces of the fibers, as shown in Figures 5 and 8(a).

Increasing the initial concentration of the 5 in these solutions resulted in the increase of their respective viscosities. This was also reflected in the location of the LDH particulates that were more permeated within the fibers than onto their surfaces. This is evident in the SEM micrographs of the LDH-PS composite fibers at a higher magnification in Figure 6. It should be also mentioned that the presence of LDH particulates into and onto the PS fibers also resulted in the deformation of the fibers, as shown in Figures 6(e) and 8(b). On the other hand, low concentration of LDH (up to 10 wt%) initially added to PS solutions containing 20 wt% of the polymer resulted in the formation of fibers with smooth surfaces and homogeneous size distribution, as shown in Figures 7 and 8(c).

The composite fibrous membranes containing the highest proportion of LDH were further analyzed for their phase composition using XRD analysis. Figure 9 shows the XRD patterns of composite fibrous membranes made of 5, 10, and 20 wt% PS containing their respective highest concentrations of LDH at 60, 40, and 10 wt%, respectively. All patterns indicated the low crystallinity of the polystyrene (PS) matrix

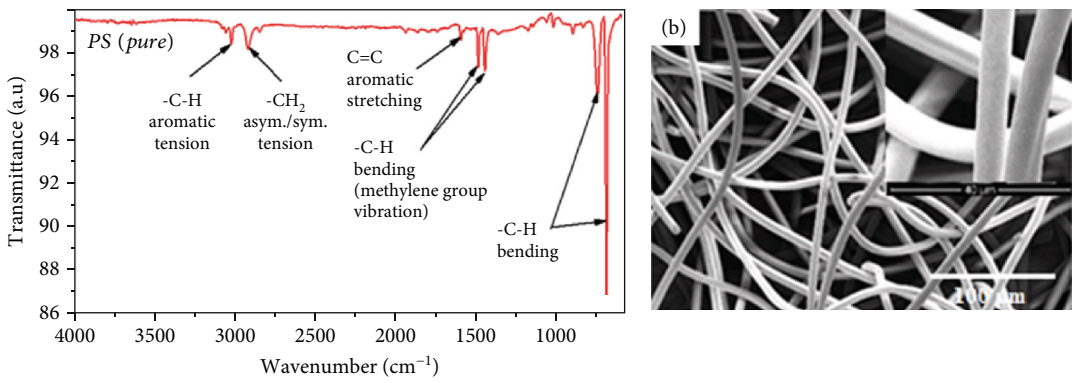

Figure 3: Infrared spectrum (a) and scanning electron micrograph (b) of the as-electrospun PS fibers. Insert in (b) is a high magnification of the PS fibers (ditto SEM in (a)).

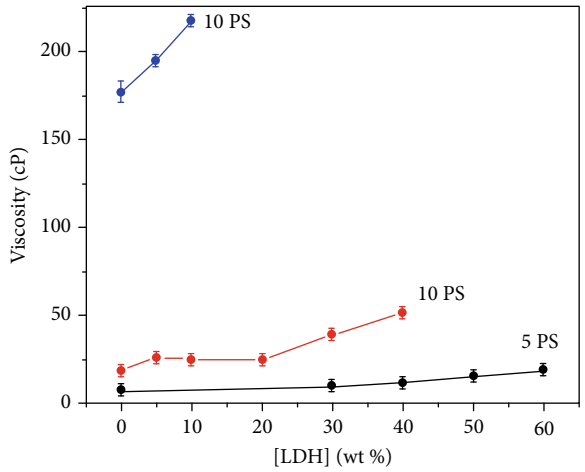

Figure 4: Variation of solution viscosity of LDH-PS mixtures as a function of initial concentration of PS and LDH particulates.

as broad peaks averaging at 10 and 19° were observed. In addition, the presence of LDH within the fibrous membranes was indicated by its main peak at 29.5°. This peak decreased in intensity when decreasing the proportion of LDH in the LDH-PS membranes. Other lower intensity peaks were also observed in the XRD pattern of the fibrous composite made of 5 wt% PS and 60 wt% LDH. It should be mentioned that the location of all peaks in their respective positions and the absence of a peak around 2° denote the absence of intercalation of the LDH sheets by the effect of the polymer during the preparation of the LDH-PS suspensions. These results are in accordance with the fact that the LDH sheets are hydrophobic while the hydrophilic hydroxyl, carbonate, or nitrate groups are entrapped between the sheets. Accordingly, the LDH particulates were enclosed within the hydrophobic PS fibers and adsorbed onto their surfaces, as shown in their respective high-magnification micrographs in Figure 8, causing an increase in the roughness of the PS fibers.

The presence of the LDH particulates within the fibrous composite membrane was further confirmed by IR and thermal analysis. Figure 10 shows the IR spectra of 5PS, 10PS, and 20PS.

PS containing their respective highest proportions of LDH particulates. IR spectra of the as-prepared LDH and PS fibers are also shown for comparison. The presence of the polystyrene (PS) fibrous matrix was confirmed by the presence of its peaks due to the stretching and bending absorptions of the C-H bonds, as marked on their spectra. On the other hand, the presence of LDH in all fibrous composites was confirmed by the presence of two bands at 3650 and 1400 cm^{-1} [52]. These are related to the $-OH^-$ and traces of the $-CO_3^{2-}$ and/or $-NO_3^-$, respectively, in the LDH-containing fibers. The intensity of these bands heightened with the increase in the proportions of LDH in the fibers. The relative intensity of the bands attributed to the interlayer anions (H_2O at 1514 cm^{-1} and nitrates and/or carbonates around 1348 cm^{-1}) in the spectra of the 5PS and 10PS containing 60 and 40 wt% LDH was reversed, when compared with their ratio in the spectrum of pure LDH. This pattern indicates a higher affinity of the LDH layers to incubate water molecules than the nitrate or carbonate groups, when enclosed within PS fibers. It also indicates that nitrates and carbonates preferentially dissolve in the polar DMF solvent, while the interlayer hydrate layer is more intact with the metal oxide layers. No further signs of chemical interaction between the LDH and PS fibers were observed, indicating the physical existence of the LDH within the composite fibrous membrane created.

The effect of the addition of LDH particulates to PS on the thermal characteristics of the produced fibrous membranes was studied by TGA and DSC techniques. Table 1 summarizes these characteristics. Thermal performance of the as-prepared LDH particulates takes place over three events: (i) the loss of interlayer hydrate molecules (100-120°C), (ii) the deformation of LDH lattice structure due to the cleavage of M-O-H bonds (300-340°C), and (iii) the formation of metal oxides by the complete conversion of hydrates to oxides in effect of thermal decomposition (470-520°C). The remaining char residue (~82%) represents the Mg and Al oxides. In contrast, the degradation of the as-electrospun PS fibers takes place until the burnout of the organic polymer leaving a 7% carbonaceous residue. It was previously shown that the higher thermal stability of LDH

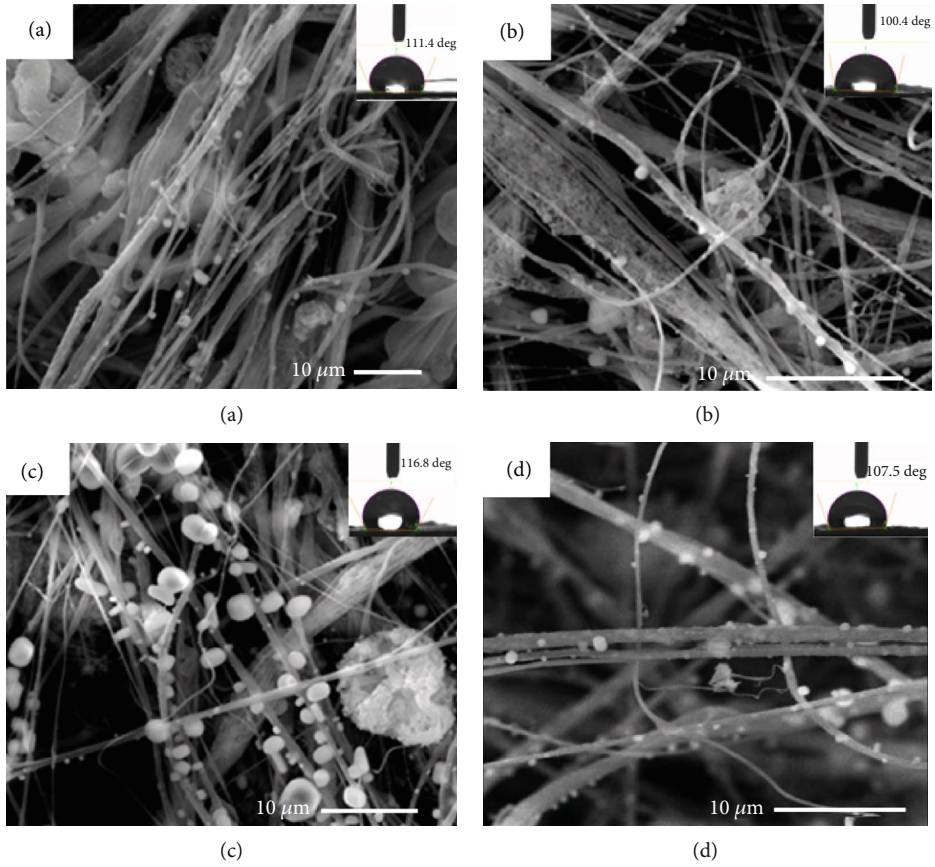

Figure 5: Scanning electron micrographs of LDH-5%PS fibrous membranes containing (a) 30%, (b) 40%, (c) 50%, and (d) 60% (by weight) LDH particulates.

enhances the thermal characteristics of the LDH-PS nanocomposites with slower decomposition rates [53]. Table 1 indicates that all LDH-PS fibrous membranes showed an enhanced thermal stability with a linear increase in the char residue with the proportion of LDH in each of the fibrous membranes. Based on the fact that no chemical reaction was proven between LDH and PS during the manufacturing of their fibrous membranes, this trend is therefore attributed to the presence of the higher thermally stable LDH component on the expense of the lower thermally stable PS matrix. Accordingly, there has been no pronounced variation in the melting point of the fibrous membranes, where an average melting point of $305.5 \pm 2.4^{\circ}C$ of the fibrous membranes was calculated. Moreover, the variation in enthalpy of melting (ΔH_m) was compared with pristine PS, indicating an increase in the latent heat energy of endothermic decomposition, due to the increase in LDH concentration within the PS matrix [54, 55]. The amount of heat energy that is required to shift the mobile phase of the polymer chain to a semicrystalline order is reduced due to the increase in the presence of crystalline LDH nucleation sites. The increasing order of LDH concentration within the composite mixture enhances the endothermic process by limiting the mobility of the polymeric chains to an ordered orientation, due to the crystalline nature of LDH layers. The increasing order of enthalpy for melting the LDH-PS composites concluded that the increase in the LDH ratio improves the latent heat of the composites, prior to thermal decomposition of the polymer matrices [55].

3.2. Evaluation of LDH and LDH-PS Fibrous Sorbents. LDH-PS fibrous membranes containing the highest proportions of LDH were evaluated for their efficiency in the sorption of Cd^{2+} ions from a simulated waste water medium as a function of time. These LDH-PS membranes were selected based on the fact that they contained the highest proportion of LDH per a given concentration of PS. Figure 11(a) shows the variation of Cd^{2+}, Mg^{2+}, and Al^{3+} ions with time for the as-prepared LDH sorbent powder. The sudden decrease in the $[Cd^{2+}]$ in the solution is accompanied by an abrupt increase in the $[Mg^{2+}]$ and a slight increase in the $[Al^{3+}]$. These results indicate a preferential exchange of the LDH-Mg ions by Cd^{2+} ions from the surrounding medium.

On the other hand, Figure 11(b) shows the concentration of Cd^{2+} ions remaining after exposure of a fixed weight of each of the LDH-PS fibrous membranes to Cd^{2+} aqueous media for up to 12 hours. In contrast, the as-prepared finely ground LDH powder sample was also evaluated. All samples showed variable abilities to remove Cd^{2+} ions from their respective media, where a sudden decrease in the $[Cd^{2+}]$ was observed to take place within the first 30 minutes of contact, indicating the fast removal of Cd^{2+} ions. This was

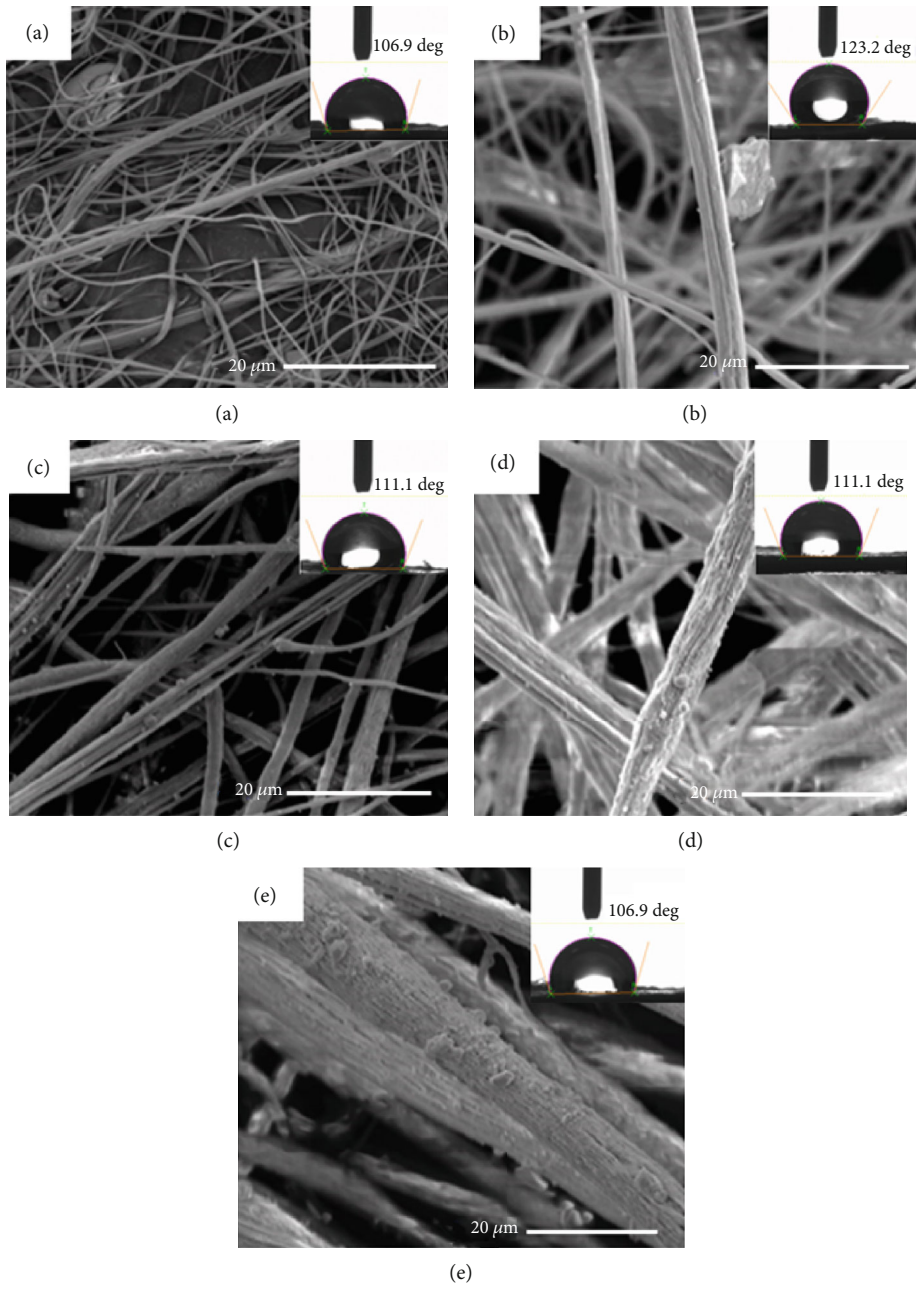

Figure 6: Scanning electron micrographs of LDH-10% PS fibrous membranes containing (a) 5%, (b) 10%, (c) 20%, (d) 30%, and (e) 40% (by weight) LDH particulates.

followed by a plateau showing a variable degree of Cd^{2+} levels remaining in the solution, indicating saturation of the samples to Cd^{2+} ions. A pure LDH sorbent showed the highest efficiency (67%) of Cd^{2+} ion removal. On the other hand, LDH-PS fibrous sorbents showed variable efficiencies of Cd^{2+} ion removal with the range of 10-15%, depending on the concentration of LDH in each of the sorbents. Due to the hydrophobicity of the PS fibrous component of the sorbents, the ability to remove Cd^{2+} ions is solely attributed to the presence of the LDH component of the sorbents, which is known to have an ion-exchange capability. The later has been extensively studied for the exchange of the interlayer of anions with other anions from the solution. A little attention has been given to the exchange of the Mg^{2+} or Al^{3+} ions by cationic species from aqueous media.

The current findings indicate the potential of fibrous membranes containing LDH to exchange its cations with Cd^{2+} in aqueous media that are highly contaminated with Cd^{2+} ions, in what is known as waste water. Accordingly, the established efficiency of removing Cd^{2+} ions under these conditions highly proposes their higher efficiency in media containing lower concentrations of Cd^{2+} ions. It should be noted that the fibrous nature of the sorbents and the interconnectivity of its intrinsic porosity facilitate the

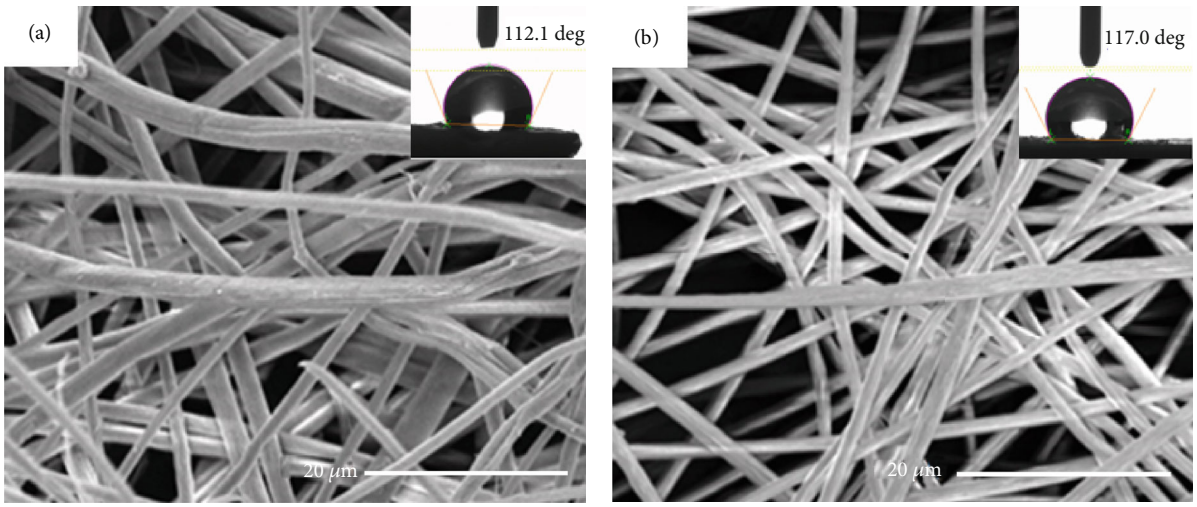

Figure 7: Scanning electron micrographs of LDH-20% PS fibrous membranes containing (a) 5% and (b) 10% (by weight) LDH particulates.

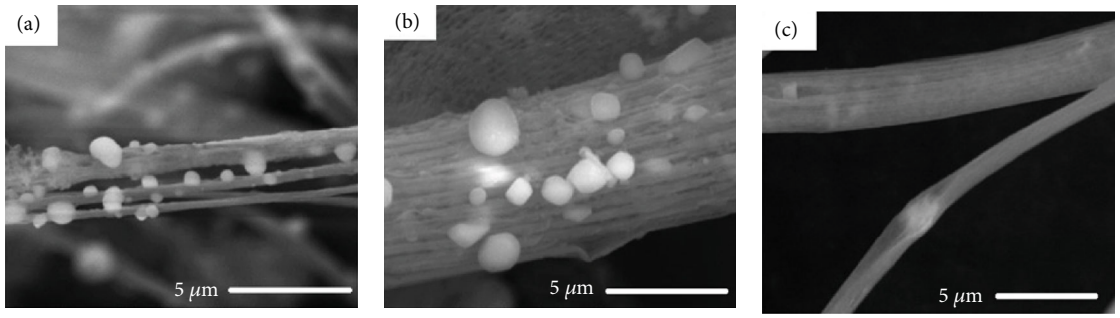

Figure 8: High-magnification scanning electron micrographs of (a) 60% LDH-5% PS, (b) 40% LDH-10% PS, and (c) 10% LDH-20% PS fibrous membranes.

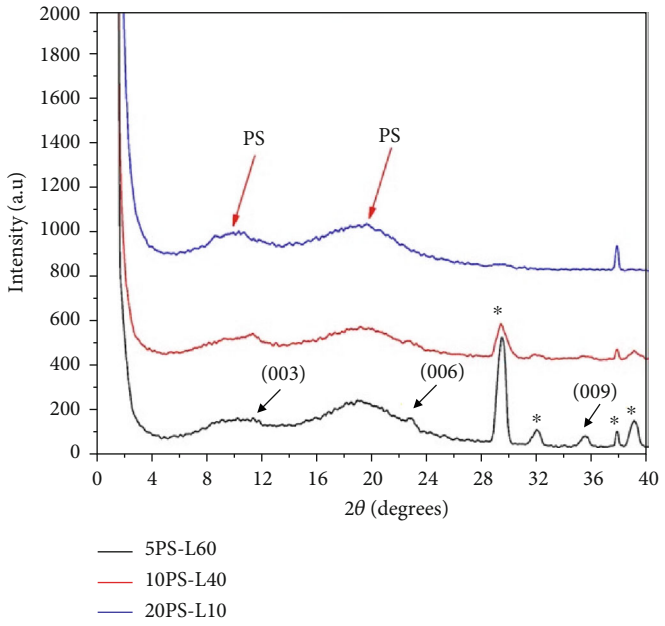

Figure 9: X-ray diffraction patterns of 60% LDH-5% PS, 40% LDH-10% PS, and 10% LDH-20% PS fibrous membranes.

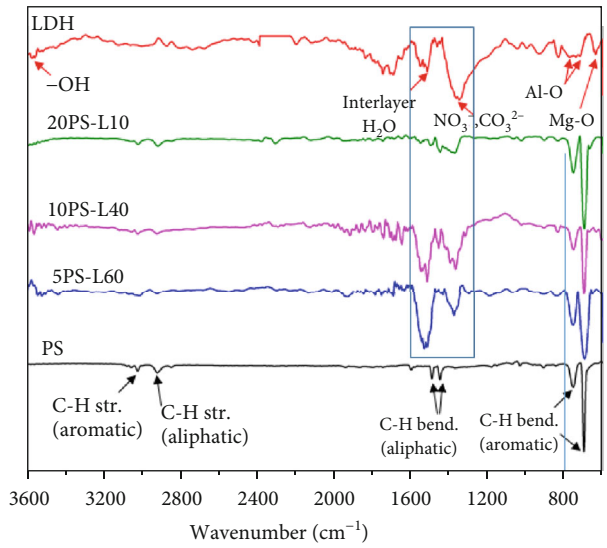

Figure 10: Infrared spectra of 60% LDH-5% PS, 40% LDH-10% PS, and 10% LDH-20% PS fibrous membranes and as-prepared LDH particulates and as-electrospun PS fibers.

Table 1: Thermal characteristics of LDH-PS fibrous membranes.

Sample	Initial temperature (°C)	Weight loss (%)	Char residue (%)	Melting temperature (T_m) (°C)	Enthalpy (ΔH_m) (J/g)
Pristine PS	284.6	93.2	7	307.1	-104.30
5PS-L30	332.1	79.8	20	306	-7.04
5PS-L40	329	76.7	23	308	-20.2
5PS-L50	336.8	74.1	26	308.2	-34.62
5PS-L60	334.3	71.1	29	308.61	-35.25
10PS-L5	340.1	91.1	9	302.2	-0.03
10PS-L10	339.1	88.4	11.6	305.6	-2.38
10PS-L20	339.6	81.5	18.5	308.7	-11.5
10PS-L30	340.1	78.6	21.4	306.4	-11.06
10PS-L40	341.3	76.7	23	306.7	-14.12
20PS-L5	327.6	90.2	10	306.4	-0.25
20PS-L10	326.5	88.5	11.5	306.6	-2.15

exposure of the LDH solid particulates to Cd^{2+} ions in solution for an exchange reaction to take place. Moreover, the hydrophobic nature of the PS fibers and the ease of its fabrication are believed to participate in the chemical stability of the PS fibrous membranes carrying the LDH particulates.

4. Conclusion

The current study investigated the formation of PS fibrous membranes containing variable proportions of MgAl-LDH particulates by an electrospinning technique. The fabricated membranes were characterized for their composition, morphology, and thermal behavior as a function of PS and LDH proportions. Selected fibrous membranes were further evaluated for their potential as ion-exchange sorbents to remove Cd^{2+} ions from water. Fibrous membranes of all compositions appeared as nonbeaded fibers with the LDH particulates incubated into and onto the surfaces of the PS fibers. Although the addition of LDH to each of the studied PS solutions increased their viscosities, there has been no indication of a chemical reaction between LDH and PS during mixing or electrospinning. In addition, mixing and electrospinning the homogeneous LDH-PS suspensions did not cause an intercalation or exfoliation of the LDH sheet structures, as proven by the XRD investigation of the fibrous membranes. However, a preferential leakage of the nitrate and carbonate ions from the LDH was evident, leaving behind a hydrate interlayer within the LDH structure. An overall improvement in the thermal characteristics of the LDH-PS fibrous membranes was observed, when compared to those of pure PS fibrous membranes. The as-prepared LDH solid particulates were proven to exchange their ions (mainly Mg^{2+} ions) with Cd^{2+} ions from aqueous media. This behavior was also shown at a lower extent in the case of PS

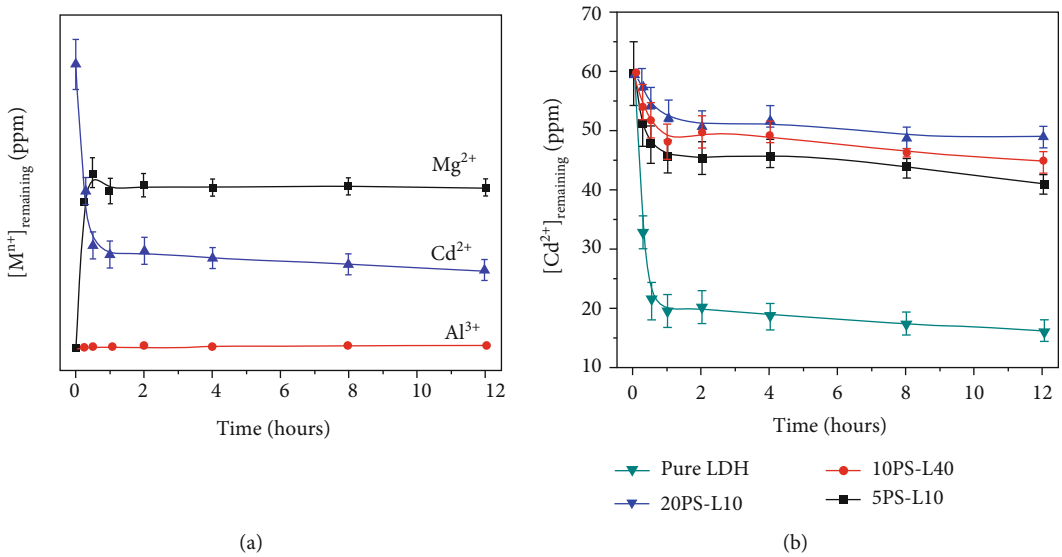

FIGURE 11: Variation of the $[Cd^{2+}]$ remaining in solution after ion exchange with LDH in (a) as-prepared LDH particulates, (b) 60% LDH-5% PS, 40% LDH-10% PS, and 10% LDH-20% PS fibrous membranes as a function of time.

fibrous membrane containing LDH particulates, due to the lower proportion of the LDH sorbent material in the membranes. It should be mentioned that the PS fibrous matrix is, therefore, an inert membrane that carries the LDH ion-exchange sorbent particulates as a water purification membrane. Accordingly, the proposed composite fibrous membrane overcomes the expected water pollution in case LDH solid particulates are directly used for water filtration. The findings of this study show the possibility of manufacturing chemically and thermally stable fibrous membrane with a potential to be used as sorbents for the removal of heavy metal ions from waste water.

Data Availability

All data presented in the manuscript are based on authentic experiments performed in our laboratories.

Conflicts of Interest

The author(s) declare(s) that they have no conflicts of interest.

Acknowledgments

This work has been supported by the kind funding of the UAE University (fund #31S316).

References

[1] A. C. Balazs, T. Emrick, and T. P. Russell, "Nanoparticle polymer composites: where two small worlds meet," *Science*, vol. 314, no. 5802, pp. 1107–1110, 2006.

[2] S. Kalia, B. Kaith, and I. Kaur, "Pretreatments of natural fibers and their application as reinforcing material in polymer composites—A review," *Polymer Engineering and Science*, vol. 49, no. 7, pp. 1253–1272, 2009.

[3] N. Cioffi, L. Torsi, N. Ditaranto, G. Tantillo, L. Ghibelli, and L. Sabbatini, "Copper nanoparticle/polymer composites with antifungal and bacteriostatic properties," *Chemistry of Materials*, vol. 17, no. 21, pp. 5255–5262, 2005.

[4] K. H. Goh, T. Lim, and Z. Dong, "Application of layered double hydroxides for removal of oxyanions: a review," *Water Research*, vol. 42, no. 6-7, pp. 1343–1368, 2008.

[5] M. Shao, F. Ning, J. Zhao, M. Wei, D. G. Evans, and X. Duan, "Preparation of Fe_3O_4@SiO_2@layered double hydroxide core–shell microspheres for magnetic separation of proteins," *Journal of the American Chemical Society*, vol. 134, no. 2, pp. 1071–1077, 2012.

[6] X. Long, Z. Wang, S. Xiao, Y. An, and S. Yang, "Transition metal based layered double hydroxides tailored for energy conversion and storage," *Materials Today*, vol. 19, no. 4, pp. 213–226, 2016.

[7] T. L. P. Galvão, C. S. Neves, A. P. F. Caetano et al., "Control of crystallite and particle size in the synthesis of layered double hydroxides: Macromolecular insights and a complementary modeling tool," *Journal of Colloid and Interface Science*, vol. 468, pp. 86–94, 2016.

[8] V. Rives, M. Del Arco, and C. J. Martín, "Layered double hydroxides as drug carriers and for controlled release of non-steroidal antiinflammatory drugs (NSAIDs): a review," *Journal of Controlled Release*, vol. 169, no. 1-2, pp. 28–39, 2013.

[9] G. Fan, F. Li, D. G. Evans, and X. Duan, "Catalytic applications of layered double hydroxides: recent advances and perspectives," *Chemical Society Reviews*, vol. 43, no. 20, pp. 7040–7066, 2014.

[10] X. Yao, D. Chungui, Y. Hua et al., "Flame-Retardant and Smoke Suppression Properties of Nano MgAl-LDH Coating on Bamboo Prepared by an In Situ Reaction," *Journal of Nanomaterials*, vol. 2019, Article ID 9067510, 12 pages, 2019.

[11] N. J. Kang, D. Y. Wang, B. Kutlu, P. C. Zhao, and A. Leuteritz, "A new approach to reducing the flammability of layered

double hydroxide (LDH)-based polymer composites: preparation and characterization of dye structure-intercalated LDH and its effect on the flammability of polypropylene-grafted maleic anhydride/d-LDH composites," *ACS Applied Materials & Interfaces*, vol. 5, no. 18, pp. 8991–8997, 2013.

[12] C. M. Becker, A. D. Gabbardo, F. Wypych, and S. C. Amico, "Mechanical and flame-retardant properties of epoxy/Mg–Al LDH composites," *Composites Part A: Applied Science and Manufacturing*, vol. 42, no. 2, pp. 196–202, 2011.

[13] V. Rives, *Layered Double Hydroxides Present and Future*, vol. 23, Nova Science Publishers Inc, NY, 2001.

[14] D. G. Evans and R. T. C. Slade, "Structural aspects of layered double hydroxides," in *Layered Double Hydroxides*, X. Duan and D. G. Evans, Eds., vol. 119 of Structure and Bonding, pp. 1–87, 2006.

[15] C. Forano, F. Bruna, C. Mousty, and V. Prevot, "Interactions between biological cells and layered double hydroxides: towards functional materials," *The Chemical Record*, vol. 18, no. 7-8, pp. 1150–1166, 2018.

[16] Z. Jiang, Z. Li, Z. Qin, H. Sun, X. Jiao, and D. Chen, "LDH nanocages synthesized with MOF templates and their high performance as supercapacitors," *Nanoscale*, vol. 5, no. 23, pp. 11770–11775, 2013.

[17] D. Sokol, K. Klemkaite-Ramanauske, A. Khinsky et al., "Reconstruction effects on surface properties of Co/Mg/Al layered double hydroxide," *Materials Science*, vol. 23, pp. 144–149, 2017.

[18] P. Z. Xu and Q. G. Lu, "Hydrothermal Synthesis of Layered Double Hydroxides (LDHs) from Mixed MgO and Al2O3: LDH formation mechanism," *Chemistry of Materials*, vol. 17, no. 5, pp. 1055–1062, 2005.

[19] S. S. Shaflei, M. Soltai-Hashjin, H. Rahim-Zadeh, and A. Samadikuchaksarei, "Synthesis and characterisation of nanocrystalline Ca–Al layered double hydroxide {$[Ca_2Al(OH)_6]NO_3.nH_2O$}: *in vitro* study," *Advances in Applied Ceramics*, vol. 112, no. 1, pp. 59–65, 2013.

[20] S. T. Qiang Wang, E. Lester, and D. O'Hare, "Synthesis of ultrafine layered double hydroxide (LDHs) nanoplates using a continuous-flow hydrothermal reactor," *Nanoscale*, vol. 5, no. 1, pp. 114–117, 2013.

[21] T. Sato, H. Fujita, T. Endo, and M. Shimada, "Synthesis of hydrotalcite-like compounds and their physico-chemical properties," *Reactivity of Solids*, vol. 5, no. 2-3, pp. 219–228, 1988.

[22] A. Du, B. Qu, Y. Meng, and Q. Zhu, "Structural characterization and thermal and mechanical properties of poly(propylene carbonate)/MgAl-LDH exfoliation nanocomposite via solution intercalation," *Composites Science and Technology*, vol. 66, no. 7-8, pp. 913–918, 2006.

[23] L. C. Du and B. J. Qu, "Structural characterization and thermal oxidation properties of LLDPE/MgAl-LDH nanocomposites," *Journal of Materials Chemistry*, vol. 16, no. 16, p. 1549, 2006.

[24] T. Kuila, H. Acharya, S. K. Srivastava, and A. K. Bhowmick, "Effect of vinyl acetate content on the mechanical and thermal properties of ethylene vinyl acetate/MgAl layered double hydroxide nanocomposites," *Journal of Applied Polymer Science*, vol. 108, no. 2, pp. 1329–1335, 2008.

[25] W. Chen and B. Qu, "LLDPE/ZnAl LDH-exfoliated nanocomposites: effects of nanolayers on thermal and mechanical properties," *Journal of Materials Chemistry*, vol. 14, no. 11, pp. 1705–1710, 2004.

[26] P. Ding and B. J. Qu, "Structure, thermal stability, and photocrosslinking characterization of HDPE/LDH nanocomposites synthesized by melt-intercalation," *Journal of Polymer Science Part B: Polymer Physics*, vol. 44, no. 21, pp. 3165–3172, 2006.

[27] G. A. Wang, C. C. Wang, and C. Y. Chen, "The disorderly exfoliated LDHs/PMMA nanocomposites synthesized by in situ bulk polymerization: the effects of LDH-U on thermal and mechanical properties," *Polymer Degradation and Stability*, vol. 91, no. 10, pp. 2443–2450, 2006.

[28] G. Camino, A. Maffezzoli, M. Braglia, M. De Lazzaro, and M. Zammarano, "Effect of hydroxides and hydroxycarbonate structure on fire retardant effectiveness and mechanical properties in ethylene-vinyl acetate copolymer," *Polymer Degradation and Stability*, vol. 74, no. 3, pp. 457–464, 2001.

[29] Q. Wang, J. P. Undrell, Y. S. Gao, G. P. Cai, J. C. Buffet, and C. A. Wilkie, "Synthesis of Flame-Retardant Polypropylene/LDH-Borate Nanocomposites," *Macromolecules*, vol. 46, no. 15, pp. 6145–6150, 2013.

[30] M. J. Solomon, A. S. Almusallam, K. F. Seefeldt, A. Somwangthanaroj, and P. Varadan, "Rheology of polypropylene/clay hybrid materials," *Macromolecules*, vol. 34, no. 6, pp. 1864–1872, 2001.

[31] O. C. Wilson Jr., T. Olorunyolemi, A. Jaworski et al., "Surface and interfacial properties of polymer-intercalated layered double hydroxide nanocomposites," *Applied Clay Science*, vol. 15, no. 1-2, pp. 265–279, 1999.

[32] G. A. Wang, C. C. Wang, and C. Y. Chen, "The disorderly exfoliated LDHs/PMMA nanocomposite synthesized by in situ bulk polymerization," *Polymer*, vol. 46, no. 14, pp. 5065–5074, 2005.

[33] W. Chen, L. Feng, and B. J. Qu, "In situ synthesis of poly(methyl methacrylate)/MgAl layered double hydroxide nanocomposite with high transparency and enhanced thermal properties," *Solid State Communications*, vol. 130, p. 259, 2004.

[34] Y. Fukushima and S. Inagaki, "Synthesis of an intercalated compound of montmorillonite and 6-polyamide," *Journal of Inclusion Phenomena*, vol. 5, no. 4, pp. 473–482, 1987.

[35] M. R. Islam, Z. Guo, D. Rutman, and T. J. Benson, "Immobilization of triazabicyclodecene in surfactant modified Mg/Al layered double hydroxides," *RSC Advances*, vol. 3, pp. 24247–24255, 2013.

[36] T. Ondarçuhu and C. Joachim, "Drawing a single nanofibre over hundreds of microns," *Europhysics Letters (EPL)*, vol. 42, no. 2, pp. 215–220, 1998.

[37] L. Feng, S. Li, Y. Li et al., "Super-hydrophobic surfaces: from natural to artificial," *Advanced Materials*, vol. 14, no. 24, pp. 1857–1860, 2002.

[38] G. Liu, X. Yan, and S. Duncan, "Polystyrene-*block*-polyisoprene Nanofiber Fractions. 2. Viscometric Study," *Macromolecules*, vol. 36, no. 6, pp. 2049–2054, 2003.

[39] B. A. Grzybowski, A. Winkleman, J. A. Wiles, Y. Brumer, and G. M. Whitesides, "Electrostatic self-assembly of macroscopic crystals using contact electrification," *Nature Materials*, vol. 2, no. 4, pp. 241–245, 2003.

[40] T.-Z. Jia, J.-P. Lu, X.-Y. Cheng et al., "Surface enriched sulfonated polyarylene ether benzonitrile (SPEB) that enhances heavy metal removal from polyacrylonitrile (PAN) thin-film composite nanofiltration membranes," *Journal of Membrane Science*, vol. 580, pp. 214–223, 2019.

[41] X. Li, L. Deng, X. Yu, M. Wang, and X. Wang, "A novel profiled core–shell nanofibrous membrane for wastewater treatment by direct contact membrane distillation," *Journal of Materials Chemistry A*, vol. 4, no. 37, pp. 14453–14463, 2016.

[42] E. A. Al Matroushi, Y. E. Greish, M. A. Meetani, and B. A. Al Shamisi, "Application of cellulose acetate fibrous membranes in the removal of micro- and submicron solid particulates in drinking water media," *Desalination and Water Treatment*, vol. 57, no. 33, pp. 15676–15686, 2016.

[43] S. Tezuka, R. Chitrakar, A. Sonoda, K. Ooi, and T. Tomida, "Studies on Selective Adsorbents for Oxo-Anions. NO_3^- adsorptive properties of ni-fe layered double hydroxide in seawater," *Adsorption*, vol. 11, no. S1, pp. 751–755, 2005.

[44] M. Zhang, B. Gao, Y. Yao, and M. Inyang, "Phosphate removal ability of biochar/MgAl-LDH ultra-fine composites prepared by liquid-phase deposition," *Chemosphere*, vol. 92, no. 8, pp. 1042–1047, 2013.

[45] J. Yu, Z. Zhu, H. Zhang, Y. Qiu, and D. Yin, "Mg–Fe layered double hydroxide assembled on biochar derived from rice husk ash: facile synthesis and application in efficient removal of heavy metals," *Environmental Science and Pollution Research*, vol. 25, no. 24, pp. 24293–24304, 2018.

[46] Y. Lee, J. H. Choi, H. J. Jeon, K. M. Choi, J. W. Lee, and J. K. Kang, "Titanium-embedded layered double hydroxides as highly efficient wateroxidation photocatalysts under visible light," *Energy & Environmental Science*, vol. 4, no. 3, pp. 914–920, 2011.

[47] X. L. Wu, L. Wang, C. L. Chen, A. W. Xu, and X. K. Wang, "Water-dispersible magnetite-graphene-LDH composites for efficient arsenate removal," *Journal of Materials Chemistry*, vol. 21, no. 43, pp. 17353–17359, 2011.

[48] X. Liang, Y. Zang, Y. Xu et al., "Sorption of metal cations on layered double hydroxides," *Colloids and Surfaces A: Physicochemical and Engineering Aspects*, vol. 433, pp. 122–131, 2013.

[49] S. Komarneni, N. Kozai, and R. Roy, "Novel function for anionic clays: selective transition metal cation uptake by diadochy," *Journal of Materials Chemistry*, vol. 8, no. 6, pp. 1329–1331, 1998.

[50] F. Liu, L. Li, P. Ling et al., "Interaction mechanism of aqueous heavy metals onto a newly synthesized IDA-chelating resin: Isotherms, thermodynamics and kinetics," *Chemical Engineering Journal*, vol. 173, no. 1, pp. 106–114, 2011.

[51] M. Park, C. L. Choi, Y. J. Seo et al., "Reactions of Cu^{2+} and Pb^{2+} with Mg/Al layered double hydroxide," *Applied Clay Science*, vol. 37, no. 1-2, pp. 143–148, 2007.

[52] B. Balcomb, M. Singh, and S. Singh, "Synthesis and characterization of layered double hydroxides and their potential as nonviral gene delivery vehicles," *Chemistry Open*, vol. 4, no. 2, pp. 137–145, 2015.

[53] Z. Matusinovic and H. Lu, "The role of dispersion of LDH in fire retardancy: the effect of dispersion on fire retardant properties of polystyrene/Ca–Al layered double hydroxide nanocomposites," *Polymer Degradation and Stability*, vol. 97, no. 9, pp. 1563–1568, 2012.

[54] Z. Matusinovic, J. Feng, and C. A. Wilkie, "The role of dispersion of LDH in fire retardancy: The effect of different divalent metals in benzoic acid modified LDH on dispersion and fire retardant properties of polystyrene– and poly(methyl-methacrylate)–LDH–B nanocomposites," *Polymer Degradation and Stability*, vol. 98, no. 8, pp. 1515–1525, 2013.

[55] K. Suresh, R. V. Kumar, and G. Pugazhenthi, "Processing and characterization of polystyrene nanocomposites based on CoAl layered double hydroxide," *Journal of Science: Advanced Materials and Devices*, vol. 1, pp. 351–361, 2016.